Published in final edited form as:

Int J Radiat Oncol Biol Phys. 2014 September 01; 90(1): 44–52. doi:10.1016/j.ijrobp.2014.05.003.

microRNA Alterations Driving Acute and Late Stages of Radiation-Induced Fibrosis in a Murine Skin Model

Brittany A. Simone, DO[*], **David Ly, MD**[†], **Jason E. Savage, MS**[†], **Stephen M. Hewitt, MD, PhD**[‡], **Tu D. Dan, MD**[*], **Kris Ylaya, MS**[‡], **Uma Shankavaram, PhD**[†], **Meng Lim, MS**[*], **Lianjin Jin, MD, PhD**[*], **Kevin Camphausen, MD**[†], **James B. Mitchell, PhD**[§], **Nicole L. Simone, MD**[*]

[*] Department of Radiation Oncology, Kimmel Cancer Center, Jefferson Medical College of Thomas Jefferson University Hospital, Philadelphia, Pennsylvania [†] Radiation Oncology Branch, National Cancer Institute, National Institutes of Health, Bethesda, Maryland [‡] Department of Pathology, National Cancer Institute, National Institutes of Health, Bethesda, Maryland [§] Radiation Biology Branch, National Cancer Institute, National Institutes of Health, Bethesda, Maryland

Abstract

Purpose: Although ionizing radiation is critical in treating cancer, radiation-induced fibrosis (RIF) can have a devastating impact on patients' quality of life. The molecular changes leading to radiation-induced fibrosis must be elucidated so that novel treatments can be designed.

Methods and Materials: To determine whether microRNAs (miRs) could be responsible for RIF, the fibrotic process was induced in the right hind legs of 9-week old CH3 mice by a single-fraction dose of irradiation to 35 Gy, and the left leg served as an unirradiated control. Fibrosis was quantified by measurements of leg length compared with control leg length. By 120 days after irradiation, the irradiated legs were 20% (P=.013) shorter on average than were the control legs.

Results: Tissue analysis was done on muscle, skin, and subcutaneous tissue from irradiated and control legs. Fibrosis was noted on both gross and histologic examination by use of a pentachrome stain. Microarrays were performed at various times after irradiation, including 7 days, 14 days, 50 days, 90 days, and 120 days after irradiation. miR-15a, miR-21, miR-30a, and miR-34a were the miRs with the most significant alteration by array with miR-34a, proving most significant on confirmation by reverse transcriptase polymerase chain reaction, c-Met, a known effector of fibrosis and downstream molecule of miR-34a, was evaluated by use of 2 cell lines: HCT116 and 1522. The cell lines were exposed to various stressors to induce miR changes, specifically ionizing radiation. Additionally, in vitro transfections with pre-miRs and anti-miRs confirmed the relationship of miR-34a and c-Met.

Reprint requests to: Nicole L. Simone, MD, Department of Radiation Oncology, Thomas Jefferson University, Kimmel Cancer Center, Bodine Center for Cancer Treatment, 111 S. 11th St, G-301G Philadelphia, PA 19107. Tel: (215) 503-0554; nicole.simone@jeffersonhospital.org.

Conflict of interest: none

Supplementary material for this article can be found at www.redjournal.org.

Conclusions: Our data demonstrate an inverse relationship with miR-34a and c-Met; the upregulation of miR-34a in RIF causes inhibition of c-Met production. miRs may play a role in RIF; in particular, miR-34a should be investigated as a potential target to prevent or treat this devastating side effect of irradiation. Published by Elsevier Inc.

Introduction

As cancer survivorship continues to grow, research must focus on ameliorating the long-term side effects of cancer therapies such as radiation (1). Radiation-induced fibrosis (RIF) is such a side effect, which can have devastating consequences for patients (2–4) and can affect many organs, leading to problems such as inadequate ventilation, decreased cardiac output, reduced range of motion, poor cosmesis, and delayed wound healing (5–7). As a result, doses of radiation administered to tumors are limited by the tolerance of the surrounding normal tissues to prevent toxicities such as fibrosis.

Although several therapeutics such as vitamin E, pentoxifylline, and pirfenidone have been used to treat RIF with some improvement in range of motion, they have had limited efficacy (8–10). More significant advances might be made if treatments could directly target the molecular alterations leading to fibrosis. Although it is known that fibrosis is caused by excess collagen and alterations in extracellular matrix (ECM), the cause of these changes has yet to be elucidated. Several inflammatory cytokines, such as transforming growth factor-β (TGF-β), interleukin-1, and tumor necrosis factor have been implicated in fibrosis induced by radiation (3, 7, 11). Fibrosis can also be thought of as a balance between pro-inflammatory and anti-inflammatory cytokines such as interleukin-10 produced by regulatory T cells (12). Other molecules not primarily associated with inflammation, but that deposit collagen include the hepatocyte growth factor receptor (HGFR) or c-Met [mesenchymal-epithelial transition factor], which is a receptor tyrosine kinase, whose only known ligand is hepatocyte growth factor (HGF). When bound by its ligand, HGF, c-Met has been shown to promote cell proliferation and angiogenesis, induce migration, and inhibit apoptosis in a host of target cells outside hepatocytes (13). This particular receptor tyrosine kinase has also been associated with wound healing and collagen production (14). Given that several different molecules are involved in the production and maintenance of fibrosis, it is postulated that fibrosis could be regulated at the transcriptional and translational level (15).

Several specific microRNAs (miRs) have been implicated in regulating fibrosis of the heart, lungs, liver, and kidney resulting from other causes (15). In this study, we sought to determine whether miRs play a role in the molecular cascade of events leading to RIF so that novel targets can be identified for the development of therapeutics.

Materials and Methods

Mice and fibrosis measurements

To induce fibrosis in an in vivo model, 9-week-old CH3 mice were treated on a protocol approved by the National Cancer Institute Animal Care and Use Committee. This protocol is a modification of a leg-contracture protocol developed by Dr Helen Stone (16). Mice were placed in a custom-made jig so that only the right hind leg of the immobilized animal was

irradiated. A single-fraction dose of 35 Gy was delivered to the right hind leg of the animal by a Therapax DXT300 x-ray irradiator (Pantak, Inc, East Haven, CT) using 2.0-mm Al filtration (300 kV peak) at a dose rate of 1.8 Gy/min (17). For further details regarding in vivo radiation, see supplemental methods (available at www.redjournal.org). The mice were killed, and tissue from the hind legs including skin, subcutaneous tissue, and muscle was collected and processed at successive time points after irradiation, including 7 days, 14 days, 50 days, 90 days, and 120 days. Details on tissue processing for molecular analysis can be found in supplemental methods (available at www.redjournal.org). The length of hind legs was measured immediately before the procurement of hind leg tissue but not measured serially because of possible elongation caused by measurement. The unirradiated leg served as the control. Degree of contracture was expressed as 100% minus length of irradiated leg divided by length of unirradiated leg.

Histopathology

Fibrosis in situ was evaluated by Movat's pentachrome stain (American Mastertech Scientific Pentachrome Kit, Lodi, CA) to delineate collagen, nucleus, elastic fibers, mucin, muscle, and fibrinoid material according to their procedural guidelines (18).

microRNA array

To determine whether miRs play a role in RIF, miR microarray analysis was performed by Exiqon according to their standard array guidelines using a miR microarray chip (v.11.– hsa, mmu & rno) containing 1940 capture probes in 4 replicates, representing 831 human miRs (Woburn, MA) using 3 distinct tissue samples per time point. Arrays were conducted by locked nucleic acid (LNA)-enhanced probes on 5 ng of total RNA after the RNA integrity and quality was assessed to ensure an RNA Integrity Number (RIN) ≥7 using the Agilent Bioanalyzer (Agilent, Santa Clara, CA). Median values of the replicate spots were background subtracted and log transformed and subjected to further analysis.

Array data processing

Raw data were quantile normalized for interarray variability. Data were preprocessed to eliminate miRs with uniformly low expression or with low expression variation (standard deviation <0.3) across the experiments, retaining 502 miRs. Average linkage hierarchical clustering (Pearson correlation, average linkage) was used to obtain clustering of the data sets. To determine whether there were genes differentially expressed between unirradiated and irradiated leg tissue, differential expression analysis was performed with significant analysis of microarrays (SAM) (19). The estimated significance levels were obtained by permutation testing, and *P* values were corrected for multiple hypotheses testing using a Benjamini and Hochberg false discovery rate (FDR) adjustment. Those miRs with FDR <0.1 were selected as significantly differentially expressed. In silico analysis was conducted with Targetscan (release 5.0) (www.targetscan.org), miRDB (www.miRDB.org) (20, 21), and the miRanda algorithm (www.microRNA.org) to determine potential downstream targets related to fibrosis. All statistical analysis was completed in the statistical packages R (www.r-project.org).

Reverse transcriptase polymerase chain reaction

Reverse transcriptase polymerase chain reaction (RT-PCR) was used to confirm alterations in miR-15a, miR-21, miR-30a, and miR-34a in tissue from both radiated and unirradiated controls. These miRs showed all of the following: a 2-fold change in expression over time, an FDR <10%, and identification by SAM plot. Technical triplicates were run of 3 biological samples from each time point with use of the TaqMan microRNA assay kit to generate cDNA (Applied Biosystems, Foster City, CA) to reverse transcribe 10 ng of RNA according to the manufacturer's instructions. cDNA was amplified and expression was quantified by the ABI-7500 real-time PCR instrument (Life Technologies, Grand Island, NY) normalizing to U6 for human cell lines and sno202 for murine samples. Results were quantified by the delta-delta CT method (22). Significance was determined by comparing the irradiated samples with time-matched controls.

In vitro experiments

To analyze the miR-34a and c-Met interaction, normal human fibroblast 1522 cells and human colon carcinoma HCT116 cells were used because pilot studies confirmed inducible expression of miR-34a (data not shown). HCT116 cells (from Dr B. Vogelstein, Johns Hopkins University, November 2008) were cultured in McCoy's 5A media with 10% fetal bovine serum, penicillin, and streptomycin (100 μg/mL). AG1522 (1522) primary fibroblasts (Coriell Institute, January 2009) were cultured in F12 media with 20% fetal bovine serum, penicillin, and streptomycin. HCT116 and 1522 cells were exposed to dimethyl sulfoxide (control), irradiation (2 Gy and 10 Gy, respectively), or doxorubicin (1 μM) because this chemotherapy is noted to cause cardiac fibrosis. Further details regarding in vitro radiation are described in supplemental methods (available at www.redjournal.org). Cell lysates were then collected 12 hours after doxorubicin exposure and 24 hours after transfection or after irradiation and analyzed for miR-34a and c-Met expression by use of an enzyme-linked immunosorbent assay kit according to the manufacturer's instructions (R&D Systems, Minneapolis, MN). Pre-miR-34a and anti-miR-34a (Life Technologies, Grand Island, NY) transfections were done with lipofectamine 2000 (Invitrogen, Grand Island, NY) to determine the effect of overexpression and knockdown of miR-34a on c-Met expression with and without exposure to 1 of the 3 stressors. Additional materials and methods for in vitro enzyme-linked immunosorbent assay and Western blotting are described in supplemental methods (available at www.redjournal.org).

Statistical analysis

Expression of target proteins and miR expression in fibrotic samples was normalized to unirradiated controls, and significance was defined at $P<.05$ using the Student t test. Error is the standard error of the mean in RT-PCR and protein expression data.

Results

Radiated leg shortens over time owing to fibrosis

On gross evaluation, irradiated legs measured significantly shorter than did unirradiated controls (Fig. 1A and B). At days 50, 90, and 120 after irradiation, the irradiated leg lengths

were 86.7%, 83.7%, and 80% of control (P=.027, P=.004, and P=.013, respectively) (Fig. 1G). On histologic examination, the gross evidence of fibrosis noted by leg shortening was directly correlated with an increase in collagen fiber deposition as shown by Movat's stain in comparison with the control legs (Fig. 1C–F).

Microarrays reveal miR signature for RIF

After comparison of unirradiated control legs at days 0 and 120 with irradiated legs at day 7, 14, 50, 90, and 120,a distinct pattern or miR signature emerged from the use of unsupervised hierarchical clustering that greatly separated the control samples (unirradiated days 0 and 120) and day 7 irradiated legs from the other samples (Fig. 2A). The maximum number of miRs demonstrating at least a 2-fold change in expression from control expression occurred on day 50 after irradiation. The number of miRs demonstrating this caliber of change decreased slightly but remained significantly elevated on day 120 after irradiation compared with day 7 after irradiation (Fig. 2B). A SAM plot was developed to identify miRs that might be specific to fibrotic changes compared with miRs that might have fluctuated by chance (Fig. 2C).

RT-PCR confirms significant changes in miR-15a, miR-30a, miR-21, and miR-34a

The miRs showing a 2-fold change in expression over time, an FDR <10%, and identified by SAM plot included miR-15a, miR-30a, miR-21, and miR-34a. Although confirmatory RT-PCR revealed some significant changes in miR-15a (Fig. 3A), miR-21(Fig. 3B),andmiR-30a(Fig. 3C),miR-34ashowedthe most significant upregulation when compared with controls (Fig. 3D) at both early and late time points (P values .0574, .051, .059, and .0093 at days 7, 14, 90, and 120, respectively). On day 120, miR-34a showed a 5-fold increase compared with unirradiated controls and therefore may be affecting downstream protein expression in pathways crucial to RIF.

miR-34a downstream targets

In silico analysis of miR 34a revealed several downstream targets associated with fibrosis: c-Met, SMAD 2/3, and CTGF. Given that c-Met has been correlated with fibrotic pathogenesis in the literature, it was further evaluated and noted to decrease in most irradiated samples, but it showed the greatest decrease in relative expression (1.17 control vs 0.75 irradiated tissue) 14 days after irradiation (Fig. 4A).

Transfection experiments confirm miR-34a and c-Met alterations in response to radiation and similar stressors

Irradiation alone caused a significant increase in miR-34a expression in both cell lines (Fig. 4B). After rescue transfection of anti-miR-34a after irradiation of the cell lines, miR-34a expression was similar to that of the unirradiated control. An inverse relationship between c-Met and miR-34a expression was noted in vitro when compared with the results from our in vivo model (Fig. 4B and C). Anti-miR-34a significantly increased c-Met and had a rescue effect on c-Met expression in both cell lines after irradiation (Fig. 4D). The same trends, notably a significant increase in miR-34a and a decrease in c-Met, were noted in both cell lines in response to exposure to alternative stressors such as doxorubicin (Fig. 4E). To assess

the effect of c-Met knockdown on the fibrotic process, we performed transfection experiments with c-Met siRNA and evaluated the expression of key profibrotic molecules. We found that 2 molecules, TGF-β1 and CTGF, were upregulated in those cells with c-Met knockdown compared with those cells receiving empty vector transfection (Fig. 4F). In addition, we found that PDGF-R is downregulated in response to c-Met knockdown. Figure E2 (available at www.redjournal.org) shows quantification of these blots.

Discussion

Radiation-induced fibrosis is a side effect of radiation therapy that can have a negative impact on a patient's quality of life during survivorship. Medical assisted devices are often used by patients with a loss of functionality caused by the development of fibrosis in muscles, nerves, or both (23). Although several studies have been conducted using antioxidants and treatments that increase vascularity and promote oxygen delivery to combat RIF, there are no specific targeted therapies or preventative agents for RIF (10, 23). This lack of targeted therapies prompted us to explore the role of miRs in the induction of RIF in an in vivo model.

In our model, it is assumed that leg shortening is caused by the fibrotic reaction that occurs in the muscle and skin within the mouse leg. Although there is no perfect model for measuring fibrosis, the leg shortening model offers a standardized method that we have used in our laboratory for many years. The initial model was described by Dr Helen Stone in this journal in 1984 and has been used in many published reports subsequently (16, 24, 25). Admittedly, measurement of fibrosis in vivo is difficult because there is no histopathologic finding that is highly sensitive or specific for RIF. Pathologic analysis reveals abundant evidence of fibrosis in the irradiated leg; however, quantification of this fibrosis remains difficult and may not correlate with clinically relevant fibrosis. Although atrophy and decreased growth may also play a role, the demonstration of increased collagen fibers within muscle suggests that the predominant cause of the observed shortening is fibrosis. Therefore, we are confident that this leg contracture model is a sufficient and reproducible model of RIF.

Four miRs were significantly altered on miR array and were worthy of further investigation; of these, miR-34a appeared to have the most significant alteration. Previous studies have implicated miR-34a in fibrosis because of its relationship to c-Met, an antifibrotic molecule, warranting further examination of this relationship (26). In our in vivo model, we were able to simulate physiologic late effects of radiation with the leg shortening model and found miR-34a upregulation even at the latest time point with concurrent decreased expression of c-Met. Studies have shown direct correlation and binding sites between miR-34a and c-Met, and an inverse relationship between them has been demonstrated (27, 28). Knockdown of c-Met is shown to increase fibrosis by the deposition of extracellular matrix (29–31) through expression of TGF-β in a Smad3-dependent manner. In the setting of chronic fibrosis, particularly in the liver, there is thought to be a balance between TGF-β and HGF (32). If the HGFR, or c-Met, is downregulated, there is no longer a balance, and TGF-β is the dominating molecule. In addition, several studies have implicated activation of c-Met in angiogenesis and activation of vascular endothelial growth factor, which is known to be

decreased particularly in RIF (33). We postulated that perhaps the use of an anti-miR34a molecule could restore c-Met expression in response to irradiation (34). We were able to show that a knockdown of c-Met in vitro results in upregulation of TGF-β and CTGF, both significant contributors to fibrosis. We noted that PDGF-R was downregulated with c-Met knockdown, which is consistent with previous literature published on Met and PDGF-R and its ligand PDGF (35, 36). This particular interaction between Met and PDGF has been associated more with epithelial cell motility than fibrosis. Our findings suggest a mechanism of crosstalk between c-Met and TGF-β and CTGF, contributing to RIF.

Radiation-induced fibrosis can take many years to develop, and there is mounting evidence demonstrating that fibrosis is a dynamic process that can be reversed; a miR-34a inhibitor could be used to increase the quality of life for patients in the survivorship phase. It has been shown that treatments such as pentoxyfylline, vitamin E, and pirfenidone, which have some efficacy in reversing RIF late after irradiation, have had no effect on the acute effects of fibrosis (10, 37, 38). Therefore, the development of clinical protocols with ideal timing of using a miR-34a inhibitor will be crucial. Its use would not be recommended during definitive treatment because c-Met has mitogenic properties and may potentiate epithelial-to-mesenchymal transformation, which could increase the risk of cancer recurrence (14).

In conclusion, future studies should examine the relationship between miR-34a and c-Met in the context of RIF. miR-34a may be a marker for radiation-induced injury (39); in addition, peptide nucleic acid or locked nucleic acid technology could be developed to create targeted inhibitors against miRs for the treatment of RIF. The sustained dysregulation of miR-34a through late stages of RIF confirms its relevance, warranting future studies to evaluate this miR as a potential marker of RIF and treatment target.

Supplementary Material

Refer to Web version on PubMed Central for supplementary material.

References

1. Tobias JS. Clinical practice of radiotherapy. Lancet 1992;339:159–163. [PubMed: 1370338]
2. Gieringer M, Gosepath J, Naim R. Radiotherapy and wound healing: Principles, management and prospects (review). Oncol Reps 2011;26: 299–307.
3. Chin MS, Freniere BB, Bonney CF, et al. Skin perfusion and oxygenation changes in radiation fibrosis. Plast Reconstr Surg 2013; 131:707–716. [PubMed: 23542244]
4. Johns MM, Kolachala V, Berg E, et al. Radiation fibrosis of the vocal fold: From man to mouse. Laryngoscope 2012;122(Suppl 5):S107–S125. [PubMed: 23242839]
5. Robbins ME, Zhao W. Chronic oxidative stress and radiation-induced late normal tissue injury: A review. Int J Radiat Biol 2004;80:251–259. [PubMed: 15204702]
6. Ghafoori P, Marks LB, Vujaskovic Z, et al. Radiation-induced lung injury. Assessment, management, and prevention. Oncology 2008;22: 37–47. discussion 52–33. [PubMed: 18251282]
7. Devalia HL, Mansfield L. Radiotherapy and wound healing. Int Wound J 2008;5:40–44. [PubMed: 18081782]
8. Jacobson G, Bhatia S, Smith BJ, et al. Randomized trial of pentoxifylline and vitamin E vs standard follow-up after breast irradiation to prevent breast fibrosis, evaluated by tissue compliance meter. Int J Radiat Oncol Biol Physics 2013;85:604–608.

9. Delanian S, Porcher R, Balla-Mekias S, et al. Randomized, placebo-controlled trial of combined pentoxifylline and tocopherol for regression of superficial radiation-induced fibrosis. J Clin Oncol 2003; 21:2545–2550. [PubMed: 12829674]
10. Simone NL, Soule BP, Gerber L, et al. Oral pirfenidone in patients with chronic fibrosis resulting from radiotherapy: A pilot study. Radiat Oncol 2007;2:19. [PubMed: 17540023]
11. O'Sullivan B, Levin W. Late radiation-related fibrosis: Pathogenesis, manifestations, and current management. Semin Radiat Oncol 2003; 13:274–289. [PubMed: 12903016]
12. Wynn TA. Cellular and molecular mechanisms of fibrosis. J Pathol 2008;214:199–210. [PubMed: 18161745]
13. Zarnegar R, Michalopoulos GK. The many faces of hepatocyte growth factor: From hepatopoiesis to hematopoiesis. J Cell Biol 1995;129: 1177–1180. [PubMed: 7775566]
14. Gentile A, Trusolino L, Comoglio PM. The Met tyrosine kinase receptor in development and cancer. Cancer Metastasis Rev 2008;27:85–94. [PubMed: 18175071]
15. Jiang X, Tsitsiou E, Herrick SE, et al. MicroRNAs and the regulation of fibrosis. FEBS J 2010;277:2015–2021. [PubMed: 20412055]
16. Stone HB. Leg contracture in mice: An assay of normal tissue response. Int J Radiat Oncol Biol Phys 1984;10:1053–1061. [PubMed: 6746346]
17. Xavier S, Piek E, Fujii M, et al. Amelioration of radiation-induced fibrosis: Inhibition of transforming growth factor-beta signaling by halofuginone. J Biol Chem 2004;279:15167–15176. [PubMed: 14732719]
18. Movat HZ. Demonstration of all connective tissue elements in a single section; pentachrome stains. AMA Arch Pathol 1955;60:289–295. [PubMed: 13248341]
19. Tusher VG, Tibshirani R, Chu G. Significance analysis of microarrays applied to the ionizing radiation response. Proc Natl Acad Sci U S A 2001;98:5116–5121. [PubMed: 11309499]
20. Wang X MiRDB: A microRNA target prediction and functional annotation database with a wiki interface. RNA 2008;14:1012–1017. [PubMed: 18426918]
21. Wang X, El Naqa IM. Prediction of both conserved and nonconserved microRNA targets in animals. Bioinformatics 2008;24:325–332. [PubMed: 18048393]
22. Livak KJ, Schmittgen TD. Analysis of relative gene expression data using real-time quantitative PCR and the 2(-delta delta c(t)) method. Methods 2001;25:402–408. [PubMed: 11846609]
23. Stubblefield MD. Radiation fibrosis syndrome: Neuromuscular and musculoskeletal complications in cancer survivors. PM R 2011;3: 1041–1054. [PubMed: 22108231]
24. Kumar S, Kolozsvary A, Kohl R, et al. Radiation-induced skin injury in the animal model of scleroderma: Implications for post-radiotherapy fibrosis. Radiat Oncol 2008;3:40. [PubMed: 19025617]
25. Xiao Z, Su Y, Yang S, et al. Protective effect of esculentoside a on radiation-induced dermatitis and fibrosis. Int J Radiat Oncol Biol Phys 2006;65:882–889. [PubMed: 16751070]
26. Giebeler A, Boekschoten MV, Klein C, et al. C-met confers protection against chronic liver tissue damage and fibrosis progression after bile duct ligation in mice. Gastroenterology 2009;137:297–308. 308. e291e294. [PubMed: 19208365]
27. Tanaka N, Toyooka S, Soh J, et al. Downregulation of microRNA-34 induces cell proliferation and invasion of human mesothelial cells. Oncol Rep 2013;29:2169–2174. [PubMed: 23525472]
28. Li N, Fu H, Tie Y, et al. Mir-34a inhibits migration and invasion by down-regulation of c-met expression in human hepatocellular carcinoma cells. Cancer Lett 2009;275:44–53. [PubMed: 19006648]
29. Mou S, Wang Q, Shi B, et al. Hepatocyte growth factor suppresses transforming growth factor-beta-1 and type III collagen in human primary renal fibroblasts. Kaohsiung J Med Sci 2009;25: 577–587. [PubMed: 19858036]
30. Marquardt JU, Seo D, Gomez-Quiroz LE, et al. Loss of c-met accelerates development of liver fibrosis in response to ccl(4) exposure through deregulation of multiple molecular pathways. Biochim Biophys Acta 2012;1822:942–951. [PubMed: 22386877]

31. Inagaki Y, Higashi K, Kushida M, et al. Hepatocyte growth factor suppresses profibrogenic signal transduction via nuclear export of smad3 with galectin-7. Gastroenterology 2008;134:1180–1190. [PubMed: 18395096]
32. Kwiecinski M, Noetel A, Elfimova N, et al. Hepatocyte growth factor (HGF) inhibits collagen I and IV synthesis in hepatic stellate cells by miRNA-29 induction. PloS One 2011;6:e24568. [PubMed: 21931759]
33. Lin YM, Huang YL, Fong YC, et al. Hepatocyte growth factor increases vascular endothelial growth factor-a production in human synovial fibroblasts through c-met receptor pathway. PloS One 2012;7:e50924. [PubMed: 23209838]
34. Wang H, Yang YF, Zhao L, et al. Hepatocyte growth factor gene-modified mesenchymal stem cells reduce radiation-induced lung injury. HumGene Ther 2013;24:343–353.
35. Yeh CY, Shin SM, Yeh HH, et al. Transcriptional activation of the Axl and PDGFR-alpha by c-Met through a ras- and Src-independent mechanism in human bladder cancer. BMC Cancer 2011;11:139. [PubMed: 21496277]
36. Derman MP, Chen JY, Spokes KC, et al. An 11-amino acid sequence from c-met initiates epithelial chemotaxis via phosphatidylinositol 3-kinase and phospholipase c. J Biol Chem 1996;271:4251–4255. [PubMed: 8626770]
37. Nieder C, Zimmermann FB, Adam M, et al. The role of pentoxifylline as a modifier of radiation therapy. Cancer Treat Rev 2005;31:448–455. [PubMed: 16225996]
38. Lefaix JL, Delanian S, Vozenin MC, et al. Striking regression of subcutaneous fibrosis induced by high doses of gamma rays using a combination of pentoxifylline and alpha-tocopherol: An experimental study. Int J Radiat Oncol Biol Phys 1999;43:839–847. [PubMed: 10098440]
39. Liu C, Zhou C, Gao F, et al. Mir-34a in age and tissue related radio-sensitivity and serum mir-34a as a novel indicator of radiation injury. Int J Biol Sci 2011;7:221–233. [PubMed: 21448283]

Summary

microRNAs may play a role in the regulation of radiation-induced fibrosis. Our study examined miR-34a and its downstream target c-Met in a murine model of radiation-induced fibrosis. We showed that radiation upregulates miR-34a, leading to c-Met downregulation that contributes to acute and late fibrosis. miR-34a represents a potential target for the prevention or treatment of radiation-induced fibrosis.

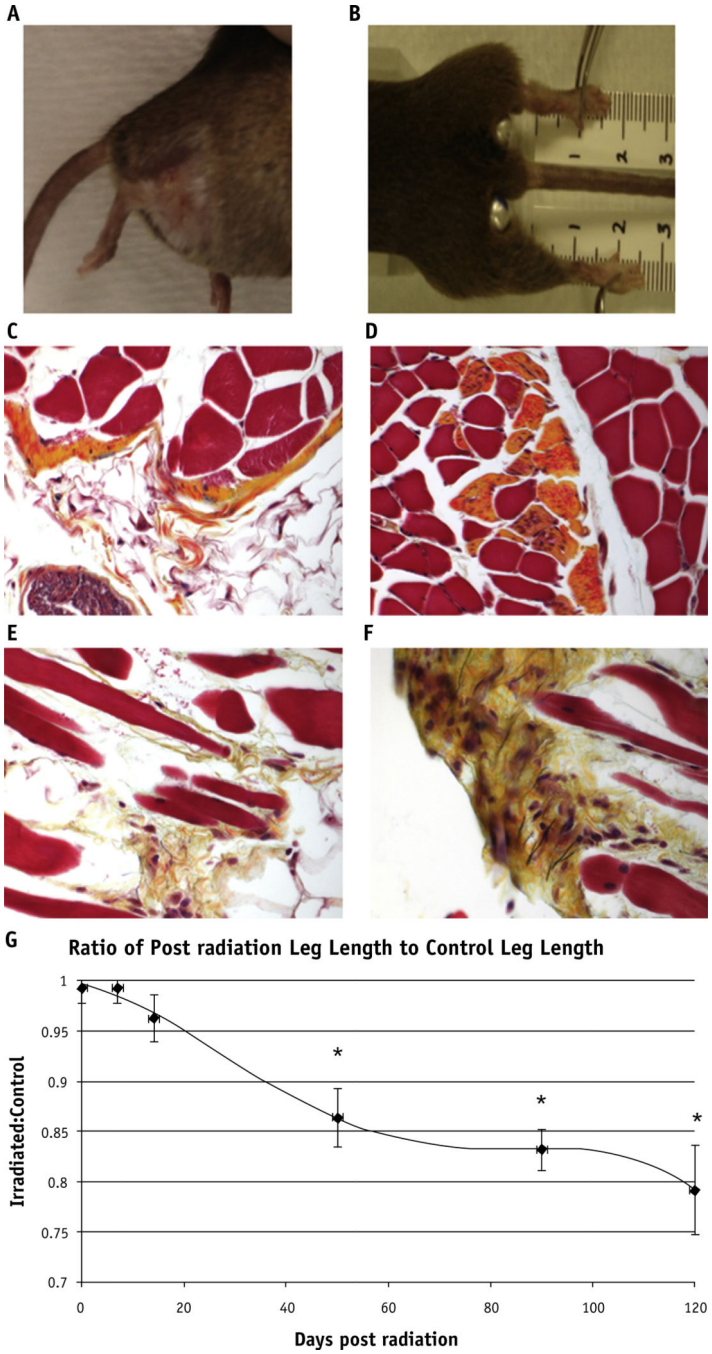

Fig. 1.

Fibrosis on gross and histologic examination. The irradiated right hind leg of a mouse has telangiectasias, alopecia, and fibrosis causing contracture at 90 days (A) and 120 days (B). Movat's pentachrome stain shows elastin fibers in black, collagen fibers in yellow, proteoglycans in blue, muscle as red, and cell nuclei as purple. Unirradiated legs (C) and (D) do not show the increased collagen deposition and excess extracellular matrix muscular atrophy, and fibrosis as seen in the irradiated legs collected at 120 days (E) and (F). (G) *Significant leg shortening effects as shown by leg measurements at later timepoints: 50

(*P*=.027), 90 (*P*=.004), and 120 days (*P*=.013) after irradiation. A color version of this figure is available at www.redjournal.org.

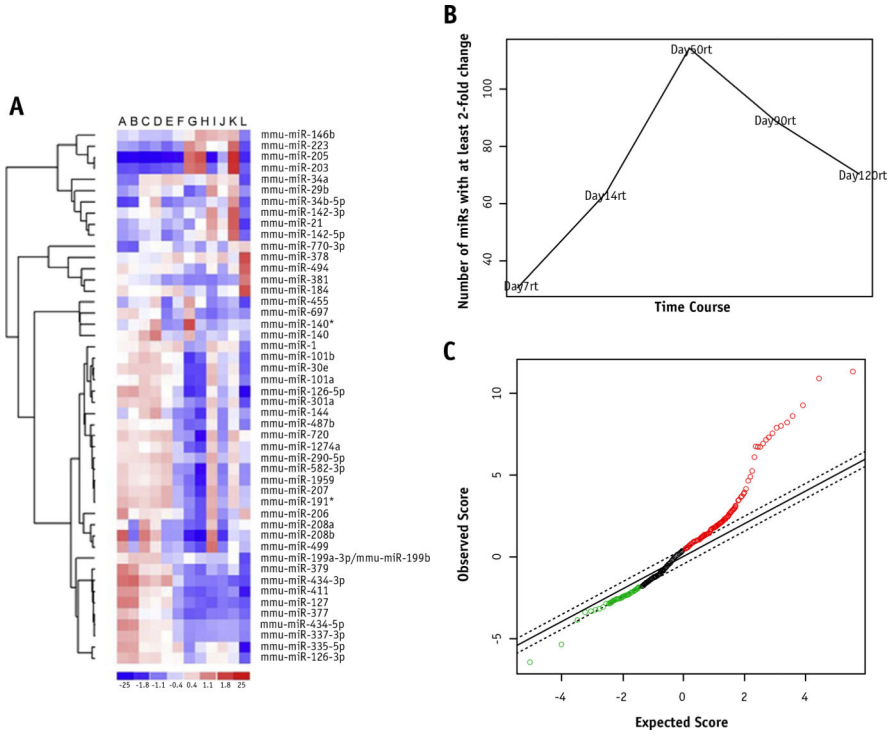

Fig. 2.

MicroRNA microarray heat map and analysis. miR arrays were performed on days 7, 14, 50, 90, and 120 after irradiation on both fibrotic and control legs. A heat map was generated to evaluate changes in miRs with a standard deviation of ≥0.5 between each time point (A); they are arranged as s from left to right: 2 day 0 controls (A and B), 7 days after irradiation (C and D), 14 days after irradiation (E), 50 days after irradiation (F and G), 90 days after irradiation (H and I), and 120 days after irradiation (J and K), and a day 120 control (L). miRs with a 2-fold change in expression (reference time-point day 0) are graphed as a function of days after irradiation (B). A significant analysis of microarrays plot was generated to help determine significantly altered miRs (C).

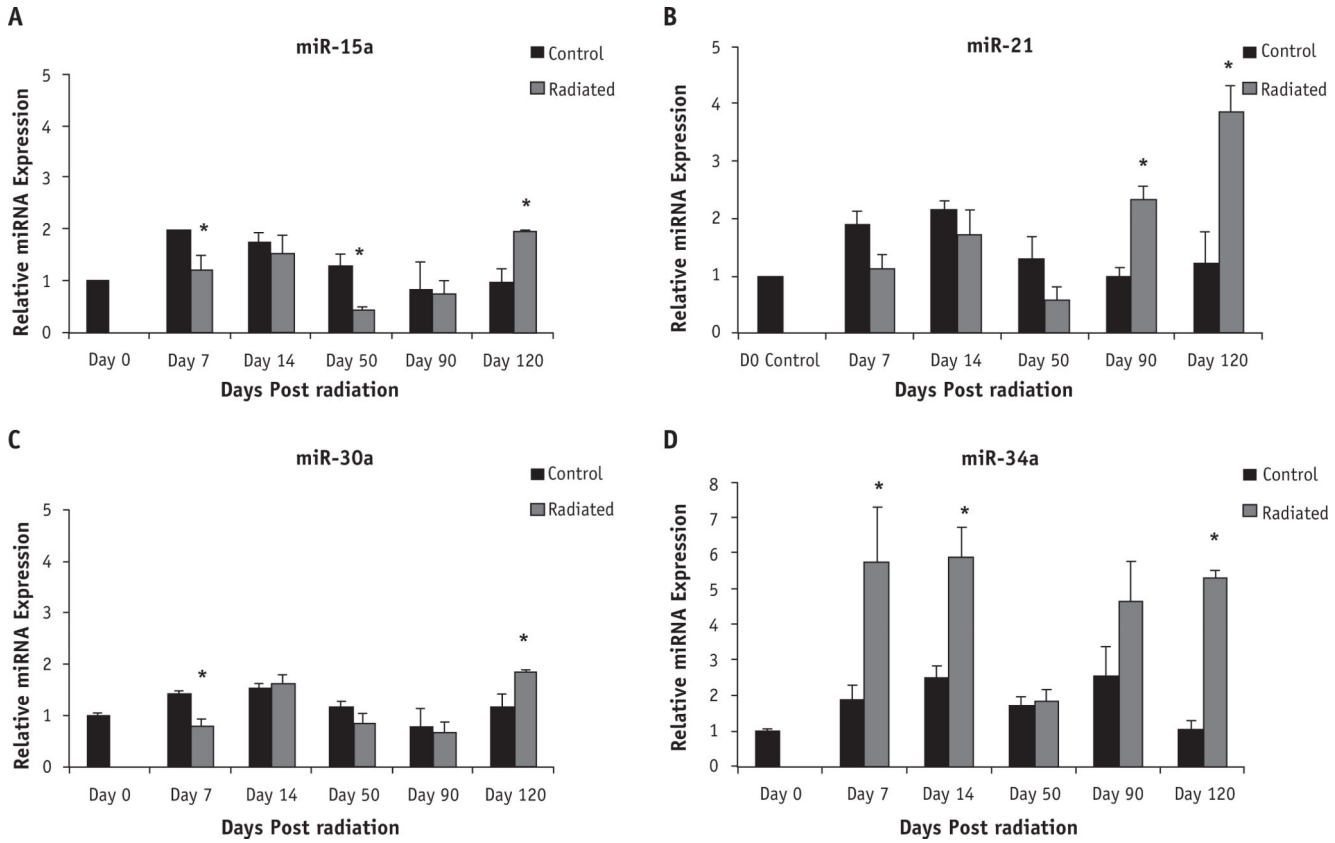

Fig. 3.

Reverse transcripitase polymerase chain reaction (RT-PCR) confirms temporal upregulation in 2 of 4 candidate microRNAs. Confirmatory RT-PCR showed few significant changes for miR-15a (A) and 30a (C) but did show several significant increases for miR-21 (B) and miR-34a (D) at day 120 (P=.0154 and P<.0001, respectively). Error bars represent standard error of the mean with biological n=5 for all microRNAs. *Significance in expression when compared with respective control.

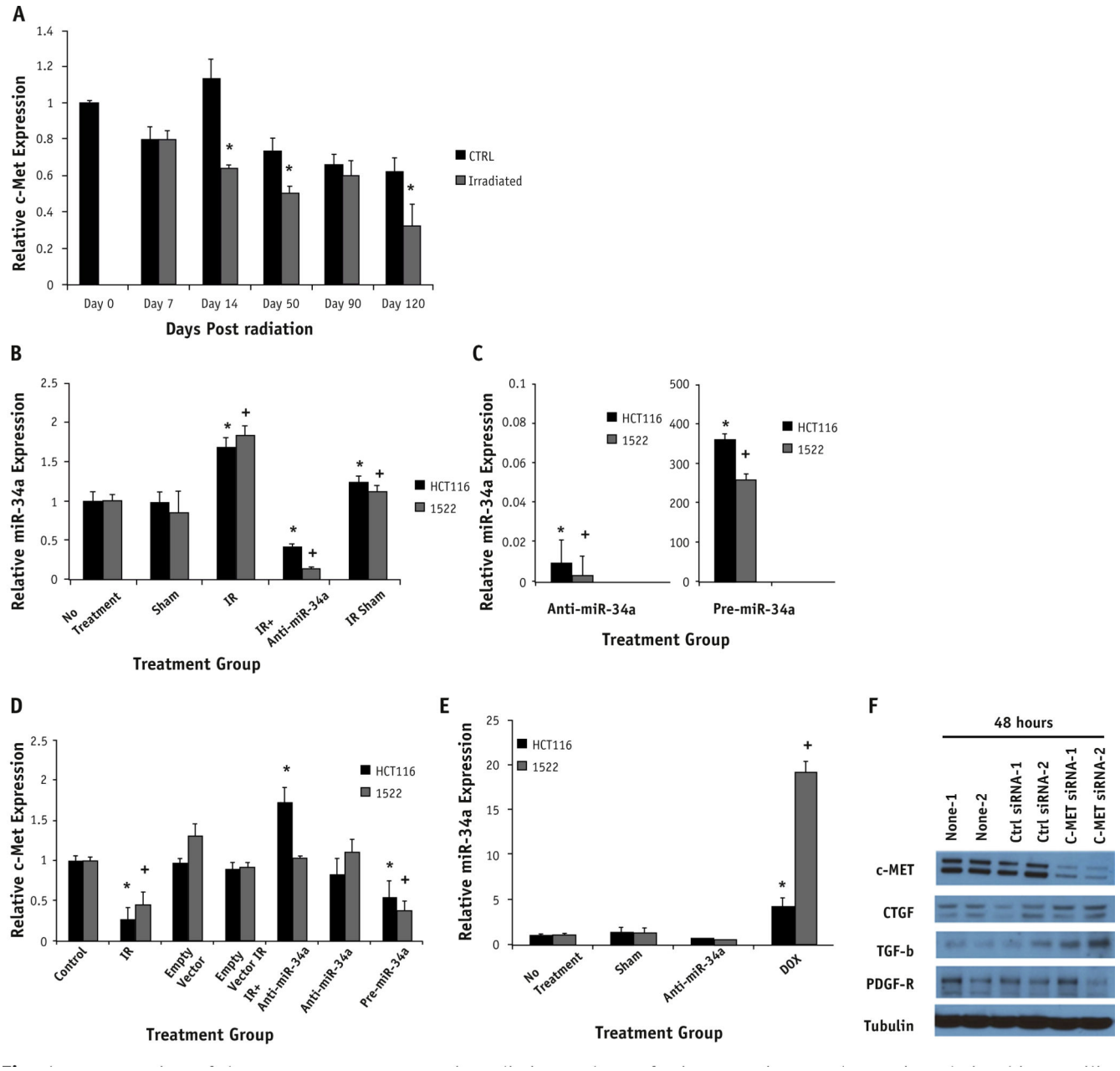

Fig. 4.

Expression of downstream target c-Met in radiation and transfection experiments show miR relationship. In silico analysis showed c-Met as a target of miR-34a and was therefore evaluated in vitro after irradiation (A). Time-points on days 14, 50, and 120 showed significantly decreased c-Met expression in comparison with time-matched controls (*P*.009, .057, and .059, respectively). Expression is normalized to the day 0 control tissue. HCT116 and 1522 cell lines (B-D) were transfected with empty vector (sham), anti-miR-34a, or pre-miR34a. Cells were also exposed to radiation (IR, 2 Gy: HCT116 and 10 Gy: 1522). Irradiation significantly increased miR-34a expression in both cell lines compared to control (CTRL) group (*P*=.024: HCT116, *P*=.011: 1522). This corresponded to

a significant decrease in c-Met expression in the same cell lines (P=.017: HCT116, P=.032: 1522). Rescue transfection with anti-miR-34a in cells exposed to irradiation restored c-Met expression (B). This correlates with the restoration of c-Met expression (D) to a level comparable with control and in HCT116 cells greater than control (P=.047). Doxorubicin-treated cells caused a similar increase in miR-34a expression (P=.001: HCT116, P<.001: 1522) (E). Significance is noted by * for HCT116 and + for 1522 cells compared with respective no-treatment cells. Anti-c-Met siRNA transfection was completed to assess response of profibrotic molecules. Knockdown of c-Met in vitro in the 1522 cell line showed c-Met to be downregulated and an upregulation of TGF-β and CTGF by Western blotting (F).